Internal and External Mass Transfer in Biofilms Grown at Various Flow Velocities

Haluk Beyenal[†] and Zbigniew Lewandowski[*,†,‡]

Center for Biofilm Engineering and Department of Civil Engineering, Montana State University, Bozeman, Montana 59717

It appears that biofilms arrange their internal structure according to the flow velocity at which they are grown, which affects the internal mass transfer rate and microbial activity. In biofilms grown at various flow velocities we determined the vertical profiles of the local relative effective diffusivity (termed D_l) at several locations within each biofilm. From these profiles we calculated the surface-averaged relative effective diffusivity (termed D_{sa}) at various distances from the bottom and plotted it against these distances. The D_{sa} decreased linearly toward the bottom, forming well-defined profiles that were different for each biofilm. The gradients of these profiles were multiplied by the diffusivity of oxygen, $\zeta = D_w\, dD_{sa}/dz$, and plotted versus the flow velocity at which each biofilm was grown. The gradients were low at flow velocities below 10 cm/s, reached a maximum at a flow velocity of 10 cm/s, and decreased again at flow velocities exceeding 10 cm/s. The existence of a maximum indicates a possibility that two opposing forces were affecting the slope of the profiles. To explain these observations we hypothesized that biofilms, depending on the flow velocity at which they are grown, arrange their internal architecture to control (1) the nutrient transport rate and (2) the mechanical pliability needed to resist the shear stress of the water flowing past them. It appears that biofilms attempt to satisfy the second goal first, to increase their mechanical strength, and that they do so at the expense of the nutrient transfer rate to deeper layers. This strength increase is associated with an increase in biofilm density, which slows down the internal mass transport rate. Biofilms grown at low flow velocities exhibit low density and high effective diffusivity but cannot resist higher shear stress, whereas biofilms grown at higher flow velocities are denser and can resist higher shear stress but have a lower effective diffusivity.

Introduction

In biofilms at a steady state, a continuity equation like eq 1

$$D_f \frac{d^2C}{dz^2} = \frac{\mu_{max} C X_f}{Y_{X/S}(K_S + C)} \tag{1}$$

has often been seen as a convenient model that describes nutrient concentration profiles. At the macroscale, microbial activity in biofilms is controlled by the rates of nutrient transport to the biofilm and within the biofilm. Equation 1 equates the biofilm activity with the internal mass transport, assuming constant effective diffusivity and constant biofilm density.

The rate of nutrient transport to the biofilm is quantified by linking the convective external mass transfer rate to the diffusive mass transport rate across the biofilm surface. Because there is no substrate consumption in the bulk solution, the flux of nutrients across the biofilm surface must be conserved, which requires that the rates of external mass transfer ($k_l(C_b - C_s)$) and internal mass transfer ($D_f(dC/dz)|_{z=L_f}$) be equal at the biofilm surface:

$$N_s = k_1(C_b - C_s) = D_f \frac{dC}{dz}\Big|_{z=L_f} \tag{2}$$

Equation 2 is often used as a boundary condition for eq 1.

To solve eqs 1 and 2, one needs to know the external mass transfer coefficient, k_l, and the effective diffusivity in the biofilm, D_f. These parameters can be evaluated experimentally or assumed. To evaluate experimentally the external mass transfer coefficient, k_l, Horn and Hempel (1997) used dissolved oxygen microelectrodes and measured oxygen profiles while operating the biofilm reactor under laminar flow conditions ($500 < Re < 2000$) and recommended the following empirical equation to calculate the Sherwood number (Sh) for biofilms:

$$Sh = 2Re^{0.5}Sc^{0.5}\left(\frac{d_h}{L}\right)^{0.5}(1 + 0.0021\ Re) \tag{3}$$

Once the Sherwood number is estimated from eq 3, the external mass transfer coefficient can be calculated as $k_l = Sh\ D_w/d_h$.

Most existing experimental procedures for measuring effective diffusivity in biofilms assume that it is constant

* Tel: (406) 994-5915. Fax: (406) 994-6098. Email: ZL@erc.montana.edu.

[†] Center for Biofilm Engineering.

[‡] Department of Civil Engineering.

10.1021/bp010129s CCC: $22.00
Published on Web 12/29/2001

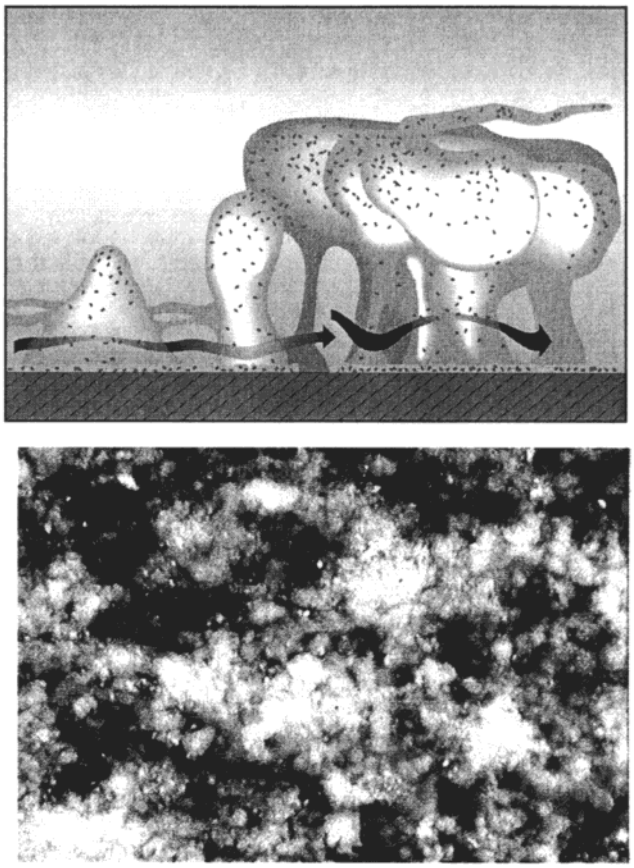

Figure 1. Heterogeneous biofilms. (Top) Diagrammatic representation of the structure of a hypothetical bacterial biofilm drawn from confocal scanning laser microscopy examination of a large number of mixed-species biofilms. A network of interstitial voids filled with water surrounds discrete microcolonies of microorganisms. The arrows indicate convective flow within the water channels. (Bottom) Light microscope image of a heterogeneous biofilm.

(Stewart, 1998; Converti et al., 1995). In a similar fashion, existing biofilm models (Cristiano et al., 2000; Picioreanu et al., 2000a,b, 1998; Wood and Whitaker, 1998; Converti et al., 1995) use a single effective diffusivity for the entire biofilm. However, Fu et al. (1994), Zhang and Bishop (1994a,b), Zhang et al. (1995), De Beer et al. (1997), Bryers and Drummond (1996), and Lawrence et al. (1994) demonstrated that effective diffusivity in biofilms varies from one location to another, probably as a result of the heterogeneous structure of biofilms: dense blocks of aggregates of biofilm microcolonies are surrounded by empty interstitial space. The nonuniform biofilm structure is likely to exhibit a nonuniform density distribution and, consequently, a nonuniform distribution of effective diffusivity. Figure 1 shows a conceptual image of such biofilms.

A high mass transfer coefficient, k_l, indicates a high nutrient transport rate, consistent with eqs 2 and 3, and implies that to increase the rate of nutrient transport to biofilms it is enough to increase flow velocity (or the Reynolds number, Re). However, such an approach is strictly mechanical and has consequences beyond those expected. Biofilms are composed of living organisms, and increasing flow velocity causes physiological responses. For example, in an extreme case, increasing flow velocity may cause sloughing of the entire biofilm. Only biofilms that are firmly attached to the surface can resist the increased shear force that is associated with increasing flow velocity.

It is well-known that biofilms grown at higher flow velocities are denser than those grown at lower flow velocities (Peyton, 1996; Gantzer et al., 1991; Characklis and Marshall, 1990). We hypothesize that this increase in biofilm density is a physiological response of the biofilm, a result of rearranging the internal biofilm structure in response to the high shear stress; denser biofilms are more likely to resist the increased shear rates associated with the high flow rates (Ohaski et al., 1999; Ohashi and Harada, 1994). However, rearranging the internal structure may affect the intrabiofilm mass transport rates. It is also expected that an increase in biofilm density may decrease the effective diffusivity in biofilms (Fan et al., 1990), which would further alter the intrabiofilm mass transport rate. Thus, increasing the flow rate in a biofilm reactor should increase the external mass transport rate, as expected, but it may also trigger a physiological response of the biofilm and change the mass transport dynamics in the biofilm in a much more complex way than that predicted by eqs 2 and 3. We initiated this work to quantify the complexity of the combined effects that flow velocity may have on growing biofilms.

Materials and Methods

To evaluate the intensity of the internal transport in biofilms, we used limiting-current-type microelectrodes to measure local effective diffusivity (Yang and Lewandowski, 1995; Beyenal and Lewandowski, 2000). The external mass transfer coefficients were evaluated using eq 3. Biofilms were grown in flat plate reactors at constant flow velocities adjusted at several preselected levels between 0.8 and 28 cm/s. When the biofilm thickness reached 250−350 μm, we interrupted the process, measured local effective diffusivity profiles across the biofilm at various locations, and estimated the average effective diffusivity. As a result, we had two sets of data for each preselected flow rate: (1) the external mass transport coefficient and (2) the effective diffusivity through the biofilm. We correlated these data with the preselected flow velocities at which the biofilms were grown and quantified the effects of flow velocity on the external mass transfer coefficient, effective diffusivity, and effective diffusivity gradients in biofilms grown at various flow velocities.

Biofilms and Biofilm Reactor. To grow biofilms we used open channel reactors similar to those described in our previous papers (Yang and Lewandowski, 1995; Beyenal et al., 1998; Beyenal and Lewandowski, 2000). These were 3.5 cm deep, 2.5 cm wide, 85 cm long, and made of polycarbonate, with a total working volume of 400 mL. The nutrient solution was made of KH_2PO_4 (0.69 mM), K_2HPO_4 (1.5 mM), $(NH_4)_2SO_4$ (0.079 mM), $MgSO_4 \cdot 7H_2O$ (0.013 mM), glucose (0.22 mM), and yeast extract (0.031 g/L). The inoculum, 1 mL of frozen stock culture (environmental isolates from the stock at the Center for Biofilm Engineering), consisted of *Pseudomonas aeruginosa* (ATCC 700829), *Pseudomonas fluorescens* (ATCC 700830), and *Klebsiella pneumoniae* (ATCC 700831).

The reactor was operated batch-wise for 12 h and then in continuous flow mode for 5−8 days until the biofilm thickness reached 250−350 μm. The biofilms were grown at various average flow velocities ranging from 0.8 to 28 cm/s. Peristaltic pumps (Cole-Parmer, Chicago, IL) were used to maintain flow and recycling of the growth medium. The system was run under a high recycle ratio (>30) to keep the nutrient concentrations constant along the reactor. The hydraulic retention time was limited to

less than 10 min in order to prevent the growth of microorganisms in the suspension. The solution was continuously aerated in a mixing chamber to keep the dissolved oxygen concentration near the saturation level in the system. Prior to use, all attachments were autoclaved at 121 °C for 20 min, and the biofilm reactor was sterilized using 70% alcohol and rinsed with sterilized distilled water. The glucose concentration in the reactor was measured using procedure 510 by Sigma Diagnostics. The dissolved oxygen concentration was monitored using a dissolved oxygen electrode.

Limiting-Current-Type Microelectrodes To Measure Local Effective Diffusivity. To measure local effective diffusivities in biofilms, we used the electrochemical technique we described previously (Beyenal et al., 1998; Beyenal and Lewandowski, 2000; Lewandowski and Beyenal, 2001). Below, we briefly describe this procedure.

Microelectrode Construction. The microelectrodes were constructed following the procedures described by Yang and Lewandowski (1995) and Beyenal et al. (1998) as redox microelectrodes with tip diameters less than 10 μm. Prior to use, each microelectrode was tested by polarizing in a solution of ferricyanide. The polarization potential was scanned from −0.2 to −1.2 V in the stagnant solution of (0.025 M) ferricyanide. Only the microelectrodes having a stable limiting current in the voltage range between −0.6 and −0.9 V were considered usable. The relation between the limiting current density and the ferricyanide concentration was linear, which confirmed that the reaction at the tip of the microelectrode was truly diffusion-controlled (Dawson and Trass, 1972).

Limiting-Current Density Measurement. Before taking the measurements, the nutrient solution in the reactor was slowly drained to ensure that the biofilm remained intact. The remaining nutrients were carefully washed from the reactor with 0.2 M KCl and replaced with an electrolyte solution made of 0.025 M $K_3Fe(CN)_6$ in 0.2 M KCl. Potassium chloride was used as a supporting electrolyte to suppress electromigration (Gao et al., 1995). This solution was recycled through the reactor for 2 h before the measurements were taken. Preparing biofilms in this manner preserved their structure but rendered them physiologically inactive (Yang and Lewandowski, 1995). We demonstrated, using microelectrodes to measure the profiles of ferricyanide and the dissolved oxygen, that neither ferricyanide nor oxygen was reduced by the biofilm under these conditions (see also Beyenal and Lewandowski, 2000; Rasmussen and Lewandowski, 1998). We used a commercial calomel electrode (model 13-620-51, Fisher Scientific, Pittsburgh, PA) as the counter/reference electrode and a Hewlett-Packard 4140B multimeter as a voltage source and picoammeter. The microelectrodes were polarized cathodically to −0.8 V against the reference electrode, and the limiting current density was calculated from the measured limiting current and the surface area of the microelectrode tip.

Calibration of the Effective Diffusivity Microelectrodes. The electrodes were calibrated in agar gels of known concentrations (from 2.5 to 100 g/L) and known effective diffusivity, measured in the diffusion cell (for details see Beyenal et al., 1998; Beyenal and Lewandowski, 2000). The limiting current density measured by the microelectrodes and the effective diffusivity calculated from the measurements in the diffusion cell were linearly correlated within the limits of tested agar densities ($R^2 = 0.97$ for 10 samples):

$$D_1 = 1.12 \times 10^{-10} + 3.69 \times 10^{-12}\, i \qquad (4)$$

Horizontal Distribution of Limiting-Current Density in Biofilms. To visualize the distribution of the effective diffusivity in the biofilm, we mapped the limiting current density at selected distances from the bottom using the position of the bottom, $z = 0$, as a reference point to determine the distance between the tip of the microelectrode and the bottom of the reactor. Before measuring the diffusivity, the biofilm reactor was positioned on an X−Y micropositioner stage (model CTC-462-2S, Micro Kinetics, Laguna Hills, CA) with the microelectrode attached to a linear micropositioner (model CTC-322-20, Micro Kinetics) and positioned above the reactor. Both micropositioners were computer-controlled through a controller (CTC-283-3, Micro Kinetics) with a positioning precision of 0.1 μm. We measured the diffusivity at the grid points of a 10 × 10 matrix with a step size of 250 μm in both X and Y directions; to start this system, the microelectrode was manually positioned above the first grid point, and the microelectrode was moved into the biofilm to the predetermined distance from the bottom. After the limiting current was measured and the data accepted, the linear micropositioner moved the microelectrode out of the biofilm into the bulk liquid, the motorized X−Y stage moved the reactor to the next grid point, and the microelectrode was lowered to the predetermined position at the same distance from the bottom as for the previous measurement.

Custom software was used to control the microelectrode movement and to monitor the limiting current. At each position of the microelectrode the data acquisition system (model CIO-DAS08PGL, Computer Boards, Inc., Mansfield, MA) collected 22 separate readings. The highest and the lowest values were trimmed, and the remaining 20 measurements were averaged. The coefficient of variation (CV) was calculated for 20 measurements and compared with the preset acceptable CV. If the measured CV was smaller than that preset, the measurement was accepted, the data were stored, and the microelectrode was moved to the next position. If the calculated CV was higher than that preset, the measurement was repeated. A relative CV of 5% was used as an arbitrary, acceptable level for all measurements. Limiting current densities measured at the same distance from the bottom were plotted to form a contour map.

Surface-Averaged and Average Effective Diffusivity Calculations. To interpret the results of microelectrode measurements we have developed the system of variables shown in Figure 2. We have explained the principles of this system previously (Beyenal and Lewandowski, 2000), but we will describe them again here for clarity.

When the local effective diffusivity (measured at a single point in the biofilm) is divided by the molecular diffusivity of ferricyanide, the result is termed the local relative effective diffusivity, D_l (Figure 2A). Using a grid of specified locations, we measured D_l at the same distance from the bottom for each point, averaged these diffusivities and termed the result surface-averaged relative effective diffusivity, D_{sa} (Figure 2B). We evaluated D_{sa} at various distances from the bottom and used this set of data to plot D_{sa} versus biofilm depth. Averaging the data from this set we obtained the average relative effective diffusivity, D_{av} (Figure 2C).

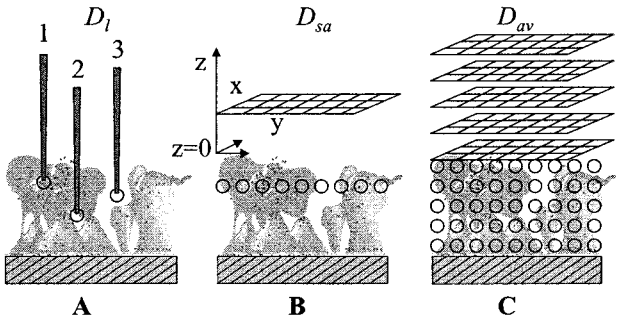

Figure 2. The system of diffusivity measurements. (A) Local relative effective diffusivity (D_l) measured by microelectrodes at arbitrarily selected locations at different distances from the bottom. (B) The D_l are measured at grid points equally distant from the bottom. The measured D_l are then averaged, which gives the surface-averaged relative effective diffusivity, $D_{sa} = \sum_{n=1}^{k} D_{l_n}/k \cdot C$) The average relative effective diffusivity, $D_{av} = \sum_{n=1}^{p} D_{sa_n}/p$, is an average of all local measurements for the entire biofilm.

To find the distribution of oxygen effective diffusivity, we multiplied the relative effective diffusivity of ferricyanide by the molecular diffusivity of oxygen and compared the effective diffusivities of oxygen with the external mass transfer coefficient (k_l) of oxygen to the biofilm. We repeated these measurement procedures for biofilms grown at several flow velocities and evaluated the effect of flow velocity on D_{sa}, D_{av}, and k_l. For each flow velocity we calculated the external mass transfer coefficients, k_l, from eq 3. The highest Re number in our system was 17,000, and we assumed that eq 3 was still valid for such high Re numbers.

The use of ferricyanide to estimate effective diffusivity in biofilms warrants explanation. Ferricyanide has a different effective diffusivity in biofilms than essential nutrients do, e.g., oxygen (Beuling et al., 2000). This is expected, as the molecular weight of ferricyanide (329) is more than 10 times higher than that of oxygen (32). The principle of our approach was to measure the effective diffusivity of ferricyanide in a biofilm and calculate the relative effective diffusivity (dimensionless) by dividing the measured effective diffusivity of ferricyanide by the molecular diffusivity of ferricyanide in water of the same temperature. This relative effective diffusivity was then assumed to be substance-independent and used to evaluate the effective diffusivities of other substances. We used it to evaluate the effective diffusivity of oxygen, by multiplying the relative effective diffusivity by the molecular diffusivity of oxygen in water. Such an approach to evaluating the effective diffusivities of various substances is generally accepted in the literature (see review by Stewart, 1998), although it should be stressed that this approach is limited to substances that (1) have similar molecular weights and (2) do not interact with the biofilm. In the case of ferricyanide, the first condition is roughly fulfilled, but the second is not; ferricyanide can be reduced by the biomass to ferrocyanide. We bypassed this problem by saturating the biofilm with the ferricyanide and waiting until the reaction was completed. Practically, the microelectrode measurements were started when the consumption of the ferricyanide by the biomass was negligible (Lewandowski and Beyenal, 2001). This approach generated an internally consistent set of data, which was then used to evaluate the effect of flow velocity on the dynamics of internal and external mass transport in biofilms.

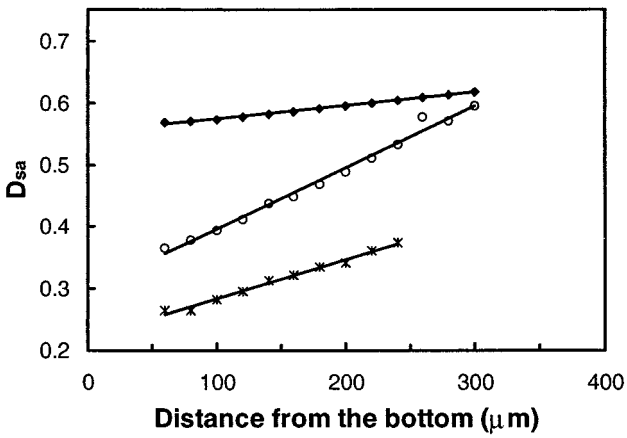

Figure 3. The D_{sa} versus the distance from the bottom for biofilms grown at some selected flow velocities: (♦) 8 cm/s; (○) 7.5 cm/s, and (*)28 cm/s.

Results and Discussion

Surface-Averaged Relative Effective Diffusivity (D_{sa}) Profiles. Figure 3 shows D_{sa} profiles measured in biofilms grown at three selected flow velocities: 0.8, 7.5, and 28 cm/s. Note that all effective diffusivity measurements were performed under stagnant conditions as described by Beyenal and Lewandowski (2000). The results in Figure 3 have been selected to demonstrate that the profiles are linear and to show trends. The complete set of data includes profiles in biofilms grown at these flow velocities: 0.8, 1.6, 3.2, 7.5, 10, 15, 20, 25, and 28 cm/s. The standard deviations from the average relative effective diffusivities (results not shown) tend to decrease toward the bottom of the biofilm because of biofilm heterogeneity (see also Beyenal and Lewandowski, 2000 for similar observations).

Each data point in Figure 3 represents an average D_{sa} value evaluated from a series of measurements at the specified distance from the bottom. The results show that biofilms grown at higher flow velocities have lower D_{sa} values than biofilms grown at lower flow velocities and at comparable distances from the bottom. This result is not surprising because we expected that the biofilms grown at higher flow velocities must have developed a stronger structure to resist the existing shear forces. As a consequence, we expected biofilms grown at higher flow velocities to be denser than biofilms grown at lower flow velocities.

It is interesting that D_{sa} values in biofilms decrease linearly toward the bottom, although at various rates depending on the flow velocity at which the biofilm was grown. The biofilms grown at low (0.8 cm/s) and high (28 cm/s) flow velocities exhibit a low slope of effective diffusivity, whereas biofilms grown at a moderate flow velocity (7.5 cm/s) have a high slope of effective diffusivity (Figure 3). Since the slope of these profiles reaches a maximum at some point, we knew to search for at least two factors (both opposite and equal to each other at moderate flow velocities) influencing the shape of the profiles in our system. In the search for these parameters we multiplied the profile slopes by the effective diffusivity of oxygen:

$$\zeta = D_w \frac{d(D_{sa})}{dz} \tag{5}$$

The product of this operation, the effective diffusivity gradient for oxygen (ζ), has the dimension of the mass transfer coefficient (length·time^{-1}), and the results in

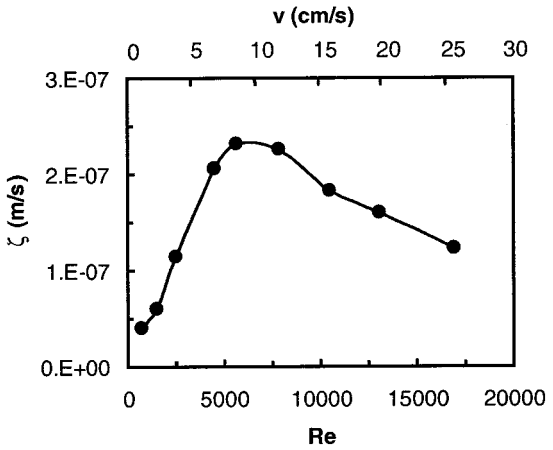

Figure 4. The diffusivity gradient, ζ (= D_w $d(D_{sa})/dz$), calculated from the data presented in Figure 3, using eq 5. The results are correlated to the Re number and flow velocity (v) at which the biofilms were grown.

Figure 4 reflect changes in the diffusivity gradient for oxygen in biofilms grown at various flow velocities.

At this point it seems that the external mass transfer coefficient in biofilms, k_l, is *directly* affected by the flow velocity, while the effective diffusivity gradient, $\zeta = D_w$ d(D_{sa})/dz, is *indirectly* influenced by the flow velocity (or perhaps more so by the Reynolds number), because the biofilms arrange their structure in response to the increasing shear forces associated with higher flow velocities. We have hypothesized that the effective diffusivity gradient in biofilms is caused by the gradient in biofilm density. In this paper, we evaluate biofilm density as dry mass (g) per unit volume (Fan et al., 1990). Biofilm density is difficult to measure without destroying the biofilm (in our case), but it can be evaluated from the effective diffusivities using the procedure proposed by Fan et al. (1990). These authors proposed the following empirical equation based on the study of many biological aggregates, including biofilms, to relate effective diffusivity and density:

$$D_{av} = 1 - \frac{0.43X_f^{0.92}}{11.19 + 0.27X_f^{0.09}} \qquad (6)$$

When the flow velocity increases, the biofilm needs to develop a stronger internal structure to resist the increasing shear force. As a result of rearranging the internal structure, its density increases, which affects the effective diffusivity (Fan et al., 1990). The most vulnerable part of the biofilm is the interface between the biofilm and the substratum, the surface at which it grows. Ohashi and Harada (1994) showed experimentally that the biofilm tensile strength increased with biofilm depth, which supports our hypothesis. Therefore, we hypothesize that as the flow velocity increases (and with it the shear force), the biofilm reinforces its structure beginning from the interface between the biofilm and the substratum, the bottom.

The maximum gradient in Figure 4 coincides with a Reynolds number of 6000, a somewhat higher Re value than traditionally assumed for the transition between laminar and turbulent flows. However, this should not be particularly surprising because we have demonstrated that the presence of biofilms in conduits may delay the onset of turbulence (Lewandowski and Altobelli, 1994). Thus, the hypothesis that the maximum diffusivity gradient coincides with the transition from laminar to turbulent flow does not disagree with our past observations.

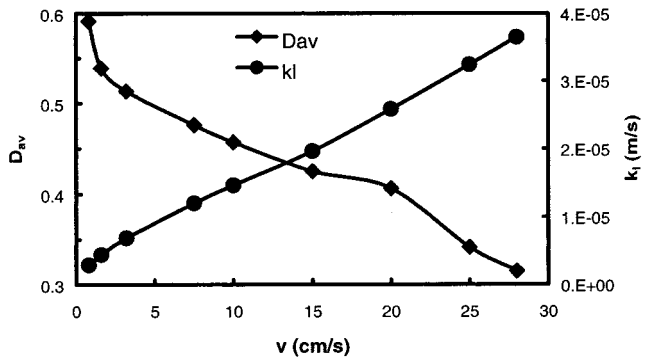

Figure 5. The average relative effective diffusivity (D_{av}) and the external mass transport coefficient (k_l) versus the flow velocity (v) at which the biofilms were grown.

Average Relative Effective Diffusivity and Mass Transport Coefficient. In Figure 5 we relate the average relative effective diffusivity (D_{av}) and the external mass transport coefficient, k_l. The results show that as the flow velocity increases, the external mass transport coefficient increases as well. However, for the same conditions the average relative effective diffusivity, D_{av}, decreases; the biofilm grown at the lowest flow velocity (0.8 cm/s) has the highest D_{av} (0.6), and the biofilm grown at the highest flow velocity (28 cm/s) has the lowest D_{av} (0.32). These D_{av} values are slightly higher than in our previous study, where they varied between 0.3 and 0.42 for flow velocities between 3.2 and 25 cm/s (Beyenal and Lewandowski, 2000). We believe that this difference is caused by differences in nutrient composition, but the extent of D_{av} variation observed in this study agrees with those reported by other authors: 0.12 to 0.88 (Livingston and Chase, 1989), 0.27 to 1 (Libicki et al., 1988), and 0.13 to 0.72 (Yano et al., 1961).

External and Internal Mass Transport in Biofilms. To better understand the nature of mass transport in our system, we calculated the Biot number, Bi = $k_l L_f/(D_{w*} D_{av})$. The Biot number (Bi) is used to compare the internal and external mass transport resistances. When Bi is large, the *external* mass transport resistance is negligible. When Bi is small, the *internal* mass transport resistance is negligible. Low mass transport resistance in biofilms translates to a concentration profile of a negligible slope. According to Bailey and Ollis (1986), if Bi is 100 or more the external mass transport resistance is negligible. In our case the Bi for oxygen was less than 100 for flow velocities less than 10 cm/s; however, for flow velocities exceeding 10 cm/sec, Bi exceeded 100. This indicates that for flow velocities less than 10 cm/s, the external mass transport resistance was limiting biofilm activity.

An acceptable strategy for overcoming the external mass transport resistance is to increase the flow velocity at which the biofilms are grown. However, our system responded to this strategy differently than was expected. In our system, increasing flow velocity increased the internal mass transfer resistance (thereby decreasing effective diffusivity). This observation is controversial because a living system should recognize the benefits of increased nutrient delivery. What the response demonstrates is that maximizing the nutrient delivery rate is only a part of the strategy that a biofilm may follow; in response to increasing flow velocity, the biofilm reinforced

its structure at the expense of nutrient delivery to the deeper layers.

A popular notion among biofilm researchers is that biofilms adjust their structure, allegedly by using cell-to-cell signaling (Davies et al., 1998), to make the structure more porous, thereby increasing the nutrient transport rate to the microorganisms located in deeper layers. We have documented here that the life strategy of biofilms can be more complex than just maximizing nutrient delivery. Our biofilms actually actively offset the benefits of increased nutrient delivery to the deeper layers to increase the internal strength, to resist shear forces, and to remain attached to the surface.

We have demonstrated (1) that effective diffusivity in biofilms varies across the biofilm and (2) that effective diffusivity in biofilms depends on the flow velocity at which the biofilms were grown. To account for these influences in modeling mass transport in biofilms we propose to rearrange the left side of the continuity equation (eq 1) by introducing variable diffusivity and diffusivity gradient:

$$D_{f_z}\frac{d^2C}{dz^2}+\zeta\frac{dC}{dz}=\frac{\mu_{max}CX_{fl}}{Y_{X/S}(K_S+C)} \qquad (7)$$

The introduced changes reflect the two conditions we propose to introduce to biofilm modeling: variable diffusivity and diffusivity gradient.

Conclusions

Mass transport in biofilms can be divided into two zones: external (from the bulk solution to the biofilm) and internal (within the biofilm). In our work, the external mass transport is characterized by the external mass transport coefficient, and the internal mass transport is characterized by the spatial distribution of the effective diffusivity. We have devised a system of measurements and calculations to evaluate the spatial distribution of the effective diffusivity, eventually averaging it at various levels within the biofilm. Following this simplification, we have shown that the effective diffusivity varies vertically within a biofilm. However, we have acknowledged the possibility of further simplifying the description of the intra-biofilm mass transport dynamics by averaging the vertically distributed effective diffusivities, and calculating an average effective diffusivity. Within this experimental system we have reached the following conclusions:

1. The effective diffusivity decreases linearly with gradient ζ toward the bottom of biofilms.

2. Increasing the flow velocity at which the biofilm grows causes the average effective diffusivity of the biofilm to decrease and the external mass transport coefficient to increase.

3. When biofilms are grown at different flow velocities, they arrange their internal structure differently, which affects the rate of internal mass transport and the rate of nutrient delivery.

4. The results indicate that biofilms adapt their internal structure to satisfy at least two goals: (i) to remain robust enough to resist shear stress and (ii) to increase the rate of nutrient delivery to deeper layers. If challenged, they appear to pursue the first goal at the expense of the second.

Acknowledgment

The research was supported by cooperative agreement EED-8907039 between the National Science Foundation and Montana State University.

Notation

Bi	Biot number ($k_lL_f/(D_{w*}D_{av})$)
C	nutrient concentration in the biofilm (kg/m^3)
C_b	bulk nutrient concentration (kg/m^3)
C_s	nutrient concentration at the biofilm surface (kg/m^3)
D	molecular diffusivity of ferricyanide in the electrolyte (m^2/s)
D_{av}	average relative effective diffusivity of ferricyanide in the biofilm
D_f	effective diffusivity of growth limiting nutrient in the biofilm (m^2/s)
D_{f_z}	surface-averaged effective diffusivity of growth-limiting nutrient in z direction (m^2/s)
d_h	hydraulic radius (m)
D_l	local relative effective diffusivity of ferricyanide in the biofilm
D_{sa}	surface-averaged relative effective diffusivity of ferricyanide
D_w	molecular diffusivity of growth limiting nutrient or oxygen (m^2/s)
i	limiting current density (ampere/m^2)
k	number of measurement points (integer)
k_l	external mass transfer coefficient (m/s)
K_s	monod half rate constant (kg/m^3)
L	length of the reactor (m)
L_f	average biofilm thickness (m)
n	integer
N_s	nutrient flux to the biofilm surface (kg/m^2/s)
Re	Reynolds number ($vd_h\rho/\mu_l$)
Sc	Schmidt number ($\rho/\mu_l/D_w$)
Sh	Sherwood number (k_ld_h/D_w)
v	flow velocity (m/s)
X_f	biofilm density (kg/m^3)
X_{fl}	surface-averaged biofilm density (kg/m^3)
$Y_{x/s}$	yield coefficient (kg microorganism/kg nutrient)
z	distance from the bottom (m)

Greek letters

ρ	density (kg/m^3)
μ_l	fluid viscosity (kg·m/s)
ζ	effective diffusivity gradient (D_wdD_{sa}/dz; m/s)
μ_{max}	maximum specific growth rate (h^{-1})

References and Notes

Bailey, J. E.; Ollis, D. F. *Biochemical Engineering Fundamentals*, 2nd ed.; McGraw-Hill: New York, 1986; pp 373−454.

Beyenal, H.; Lewandowski, Z. Combined effect of substrate concentration and flow velocity on effective diffusivity in biofilms. *Water Res.* **2000**, *34*, 528−538.

Beyenal, H.; Tanyolaç, A.; Lewandowski, Z. Measurement of local effective diffusivity and cell density variations in heterogeneous biofilms. *Water Sci. Technol.* **1998**, *38*, 171−178.

Beuling, E. E.; van den Heuvel, J. C.; Ottengraf, S. P. P. Diffusion coefficients of metabolites in active biofilms. *Biotechnol. Bioeng.* **2000**, *67*, 53−60.

Bryers, D. J.; Drummond, F. Local mass transfer coefficients in bacterial biofilms using fluorescence recovery after photobleaching (FRAP). In *Progress in Biotechnology 11, Immobilized Cell: Basics and Applications*; Wijffels, R. H., Buitelaar, R. M., Bucke, C., Tramper, J., Eds.; Elsevier: New York, 1996; pp 196−204.

Characklis, W. G.; Marshall, K. C. *Biofilms*; Wiley: New York, 1990; pp 397−443.

Converti, A.; Casagrande, M.; De Giovanni, M.; Rovatti, M.; Del Borghi, M. Evaluation of glucose diffusion coefficient through cell layers for the kinetic of an immobilized cell bioreactor. *Chem. Eng. Sci.* **1995**, *51*, 1023−2026.

Cristiano, N.; Prasert, P.; Livingston, A. G. Substrate counter diffusion and reaction in membrane-attached biofilms: Mathematical analysis of rate-limiting mechanisms. *Chem. Eng. Sci.* **2000**, *55*, 1385−1398.

Dawson, A. D.; Trass, O. Mass transfer at rough surfaces. *J. Heat Mass Transfer* **1972**, *15*, 1317−1336.

Davies, D. G.; Parsek, M. R.; Pearson, J. P.; Iglewski, B. H.; Costerton, J. W.; Greenberg, E. P. The involvement of cell-to-cell signals in the development of a bacterial biofilm. *Science* **1998**, *280*, 295−298.

De Beer, D.; Stoodley, P.; Lewandowski, Z. Measurement of local diffusion coefficients in biofilms by microinjection and confocal microscopy. *Biotechnol. Bioeng*, **1997**, *53*, 151−158.

Fan, L. S.; Ramos, R. L.; Wisecarver, K. D.; Zehner, B. J. Diffusion of phenol through a biofilm grown on activated carbon particles in a draft-tube three-phase fluidized bed bioreactor. *Biotechnol. Bioeng.* **1990**, *35*, 279−286.

Fu, Y. C.; Zhang, T. C.; Bishop, P. L. Determination of effective oxygen diffusivity in biofilms grown in a completely mixed biodrum reactor. *Water Sci, Technol.* **1994**, *29*, 455−462.

Gantzer, C. J.; Rittmann, B. E.; Herricks, E. E. Effects of long-term water velocity changes on streambed biofilm activity. *Water Res.* **1991**, *25*, 15−20.

Gao X.; Lee, J.; White, H. S. Natural convection at microelectrodes. *Anal. Chem.* **1995**, *67*, 1541−1545.

Horn, H.; Hempel, D. C. Substrate utilization and mass transfer in an autotrophic biofilm system: Experimental results and simulation. *Biotechnol. Bioeng.* **1997**, *53*, 363−371.

Lawrence, J. R.; Wolfaardt, G. M.; Korber, D. R. Determination of diffusion coefficients in biofilms by confocal laser microscopy. *Appl. Environ. Microbiol.* **1994**, *60*, 1166−1173.

Lewandowski, Z.; Beyenal, H. Limiting-current-type microelectrodes for quantifying mass transport dynamics in biofilms. In *Methods in Enzymology*; Doyle, R. J., Ed.; Academic Press: New York, 2001; Vol. 331, pp 339−359.

Lewandowski, Z.; Altobelli, S. 1994. Water flow in a narrow conduit covered with biofilm. Proceedings of the International Association on Water Quality Research Seminar "Biological Degradation of Organic Chemical Pollutants in Biofilm Systems", 19−21 May 1994, Kollekolle, Copenhagen, Denmark, paper no. 19.

Libicki, S. B.; Salmon, P. M.; Robertson, C. R. The effective diffusive permeability of a nonreacting solute in microbial cell aggregates. *Biotechnol. Bioeng.* **1988**, *32*, 68−85.

Livingston, A. G.; Chase, H. Modeling of phenol biodegradation in a fluidized-bed bioreactor. *AIChE J*. **1989**, *35*, 1980−1992.

Ohashi, A.; Harada, H. Adhesion strength of biofilm developed in an attached growth reactor. *Water Sci. Technol*. **1994**, *29*, 281−288.

Ohashi, A.; Takashi, K.; Kazuaki, S.; Harada, H. A novel method for evaluation of biofilm tensile strength resisting erosion. *Water Sci. Technol.* **1999**, *39*, 261−268.

Peyton, B. M. Effects of shear stress and substrate loading rate on *Pseudomonas aeruginosa* biofilm thickness and density. *Water Res.* **1996**, *30*, 29−36.

Picioreanu, C.; van Loosdrecht, M. C. M.; Heijnen, J. J. Mathematical modeling of biofilms structure with a hybrid differential−discrete cellular automaton approach. *Biotechnol. Bioeng.* **1998**, *58*, 101−116.

Picioreanu, C.; van Loosdrecht, M. C. M.; Heijnen, J. J. A theoretical study on the effect of surface roughness on mass transport and transformation in biofilms. *Biotechnol. Bioeng.* **2000a**, *68*, 536−547.

Picioreanu, C.; van Loosdrecht, M. C. M.; Heijnen, J. J. Effect of diffusive and convective substrate transport on biofilm structure formation: A two-dimensional modeling study. *Biotechnol. Bioeng.* **2000b**, *69*, 504−515.

Rasmussen, K.; Lewandowski, Z. Microelectrode measurements of local mass transport rates in heterogeneous biofilms. *Biotechnol. Bioeng.* **1998**, *59*, 302−309.

Stewart, P. A review of experimental measurements of effective diffusive permeabilities and effective diffusion coefficients in biofilms. *Biotechnol. Bioeng.* **1998**, *59*, 261−272.

Wood, B. D.; Whitaker, S. Diffusion and reaction in biofilms. *Chem. Eng. Sci.* **1998**, *53*, 397−425.

Yang, S.; Lewandowski, Z. Measurement of local mass transfer coefficient in biofilms. *Biotechnol. Bioeng.* **1995**, *48*, 737−744.

Yano, T.; Kodama, T.; Yamada, K. Fundamental studies on the aerobic fermentation. Part VII. Oxygen transfer within a mold pellet. *Agric. Biol. Chem.* **1961**, *25*, 580−584.

Zhang, T. C.; Bishop, P. L. Evaluation of tortuosity factors and effective diffusivities in biofilms. *Water Res.* **1994a**, *28*, 2279−2287.

Zhang, T. C.; Bishop, P. L. Density, porosity, and pore structure of biofilms. *Water Res.* **1994b**, *28*, 2267−2277.

Zhang, T. C.; Fu, Y. C.; Bishop, P. L.; Kupferle, M.; Fitzgerald, S.; Jiang, H. H.; Harmer, C. Transport and biodegradation of toxic organics in biofilms. *J. Hazard. Mater.* **1995**, *41*, 267−285.

Accepted for publication October 10, 2001.

BP010129S